



Contents lists available at ScienceDirect

Journal of Cleaner Production

journal homepage: www.elsevier.com/locate/jclepro

Experimental investigation on the feasibility of dry and cryogenic machining as sustainable strategies when turning Ti6Al4V produced by Additive Manufacturing

A. Bordin*, S. Sartori, S. Bruschi, A. Ghiotti

Dept. of Industrial Engineering, University of Padova, Via Venezia 1, 35131, Padova, Italy

ARTICLE INFO

Article history:

Received 23 July 2015

Received in revised form

13 September 2016

Accepted 28 September 2016

Available online xxx

Keywords:

Ti6Al4V

Additive Manufacturing

Sustainable machining

Cryogenic machining

Electron beam melting

ABSTRACT

The performances of the cutting fluids have recently been under investigation to drive machining operations towards cleaner and more sustainable targets. Several efforts are being made to test new formulations of coolants and to implement cooling strategies alternative to standard flooding. Cryogenic cooling seems to be an efficient solution to enhance the process sustainability when machining difficult-to-cut metals, such as nickel, cobalt and titanium alloys. Among its several advantages, no contaminants are left on the chips and workpieces, hence reducing the chips disposal costs and limiting skin and breath diseases for the machine tool operators. Furthermore, in case of production of surgical prostheses, it can help reducing the cleaning steps before the final sterilization. The present work investigates the feasibility of using dry cutting and cryogenic cooling in semi-finishing turning of the Ti6Al4V titanium alloy produced by the Additive Manufacturing technology known as Electron Beam Melting when compared to standard flood cooling. For this purpose, the effects of the cutting speed and feed rate on the tool wear, surface integrity, and chip morphology were investigated as a function of the applied cooling strategy. The experimental findings show that the cryogenic cooling assures better performances than dry and wet machining by reducing the tool wear, improving the surface finish and the chip breakability, whereas dry cutting provokes more surface defects and severe tool wear. Therefore, from an environmental point of view, cryogenic machining can represent a sustainable process for manufacturing surgical prostheses made of AM titanium alloys.

© 2016 Elsevier Ltd. All rights reserved.

1. Introduction

In the recent years, the concept of sustainable manufacturing has become of great interest within the international community due to the stricter and stricter regulations imposed by the international agreements that impose a greener and more sustainable mentality to companies operating in different industrial fields.

Since the United Nations Conference on Environment and Development (UNICED, 1992) the concept of sustainable production has become crucial to achieve a global sustainable development, promoting the creation of links between the technology and the economy driven together by the unique main goal of a green world. Since nineties, new government bodies dedicated to environmental issues have been born across Europe and US, and global

targets have been set against environmental pollution. The National Council for Advanced Manufacturing (NACFAM) is helping American industries to shift towards a more sustainable production by closing their supply chain loops, driving through industrial ecology and creating business opportunities within the sustainable manufacturing paradigm. The US Environmental Protection Agency (EPA) is providing the industrial market of many instruments to monitor and improve the processes sustainability. Among the most important environmental targets set for the evolution of the manufacturing processes, Horizon 2020 has pointed the target of 20% reduction in the EU greenhouse gas emissions from 1990 levels, the rise to 20% of the share of EU energy consumption produced from renewable resources, as well as a 20% improvement in the EU energy efficiency (Pusavec et al., 2014).

A sustainable production can be achieved by the application of sustainable principles to manufacturing, such as a green supply chain, life-cycle assessments methods,; accordingly, designers, manufacturers and process engineers must go through specific

* Corresponding author.

E-mail address: bordin.alberto.dii@gmail.com (A. Bordin).

strategies depending on the products to develop and produce. On the basis of these considerations, if the manufacturing process of metallic prostheses is considered, many phases and technical aspects along their production chain have to be investigated to improve the sustainability of the entire process.

Recently, several companies that operate in the biomedical field are investing significant resources in Additive Manufacturing (AM) technologies, such as Electron Beam Melting (EBM) and Direct Melting Laser Sintering (DMLS) (Gao et al., 2015), increasingly leaving the traditional production strategies that consist in forging or casting raw geometries followed by machining and grinding to obtain the final shapes.

The AM techniques significantly cut the costs related to material waste, initial prototyping and product transportation. Thanks to the production-on-demand, there is no need for massive product inventory, the obtained products are near-net-shape; thus further costs and material waste are reduced, but the quality of the traditionally manufactured products is preserved (Baumers et al., 2015). Nonetheless, when the 3-D printed parts are removed from the build plate, they present rough and porous surfaces that may need to be finished by machining, grinding and polishing processes. At the end of the manufacturing process, the prostheses are subjected to mandatory cleaning and sterilizing operations to remove all the pollutants and debris that remain attached and entrapped into the porous surfaces (Chen and Thouas, 2015). During this stage, the finished products are washed into special designed sterilisers that absorb a significant amount of electrical energy, consume water and chemical reagents, and increase the time required to complete the operation. Therefore, the dirtier the prosthesis the higher the energy consumption required for the cleaning steps.

Most of the prostheses available in the market are made of titanium and cobalt alloys, such as the Ti6Al4V and the F75 CoCrMo, which are characterized by a poor machinability (Shao et al., 2013) that forces to an extensive use of cutting fluids with the aim of preserving the component surface integrity and limiting the tool wear. Being the adopted cutting fluids primarily made of water emulsions, once the aqueous portion evaporates, residual chemical elements (i.e. sulphur, phosphorus, zinc,...) remain onto the workpiece, being some of them toxic for the human body (Bennett, 1983).

Moreover, the applied cutting fluid significantly affects the sustainability of machining processes (Debnath et al., 2014), being considered one of the main environmental hazards in the context of manufacturing (Dudzinski et al., 2004). In fact, the conventional semi-synthetic cutting fluids are not biodegradable; moreover, they may contain contaminants, such as heavy metals (lead, chromium, nickel), PCB, polycyclic aromatic hydrocarbons that are extremely hazardous for the human health. Furthermore, such fluids can damage water and soil resources when wrongly handled, imposing rigid and expensive disposal procedures to the manufacturing companies (Hosseini Tazehkandi et al., 2014). In addition, a prolonged exposure of the operators to standard emulsion coolants is scientifically proved to cause serious skin and breathe illnesses (Ozcelik et al., 2011).

With the goal of increasing the entire process sustainability when manufacturing AM prostheses made of Ti6Al4V as well as respecting the stricter and stricter regulations in terms of healthy work places, cleaner and greener cooling strategies have been employed to reduce the prostheses cleaning costs and the disposal costs for the used cutting fluids. According to the latest researches, dry, near dry and cryogenic cooling strategies are emerging as efficient alternatives to standard flood cooling in machining (Debnath et al., 2014). Dry machining means no cutting fluids applied during the process, thus no problems of contamination, disposal and pollution of water and air are potentially encountered.

On the other side, if dry machining is applied to difficult-to-cut alloys such as the Ti6Al4V, metallurgical alterations of the machined workpiece and severe tool wear may generate (Ezugwu and Wang, 1997). Nonetheless, if the material removal rate is low as for AM parts, dry machining might substitute the conventional flooding as proved by (Devillez et al., 2011), who found values of the micro-hardness, residual stresses and surface roughness in dry semi-finishing turning of Inconel 718 comparable to those obtained in wet turning. Near-dry machining consists of applying a very small amount of cutting fluid (up to 100 ml h⁻¹), delivered in a compressed air stream, directed at the cutting zone (Fratila, 2010). When compared to dry machining, this cooling technique enhances the machined surface integrity, improves the tool life by limiting the tool wear, also in case of machining difficult-to-cut alloys (Weinert et al., 2004). Even though near-dry machining is undoubtedly cleaner than traditional flooding, some residual oil particles are left on the workpieces and, in the case of biomedical applications, they need to be completely removed. This problem can be overcome if cryogenic machining is employed, which consists in the application of high-pressure low-temperature liquids, as the Liquid Nitrogen (LN₂) or the Liquid Carbon Dioxide (LCO₂), to the cutting zone, through external nozzles, modified commercial tool holders or newly designed systems (Yildiz and Nalbant, 2008). Since the significant reduction of the tool wear is the main beneficial effect of cryogenic cooling thanks to the drastic decrease of the cutting temperature, almost all of the works present in literature deals with applications in the field of rough machining of difficult-to-cut metals (Hong et al., 2001). In addition to that, thanks to the evaporation of the cryogenic fluid once in contact with the cutting interfaces, both the chips and the workpiece are left dry and clean after the machining process, fulfilling the goals of reducing the costs for disposing the used cutting fluids as well as the costs for the cleaning steps, thus achieving a cleaner process chain in comparison with standard flooding (Pusavec et al., 2010).

On the basis of these considerations, dry and cryogenic machining can be implemented as clean strategies to the finishing turning and milling of AM Ti6Al4V prostheses. Since no works are present in literature about this topic, the presented research is aimed at proving the feasibility of applying dry and cryogenic cooling strategies when semi-finishing turning the Ti6Al4V titanium alloy produced by the EBM technology. A comparison with a standard flood cooling is given, focusing the investigation on the tool wear, machined surface integrity, and chip morphology.

2. Experimental work

2.1. Workpiece material

The alloy tested in the present work is the Ti6Al4V titanium alloy manufactured by the Electron Beam Melting (EBM) Additive Manufacturing (AM) process. The material was supplied in 4 round cylindrical specimens printed along their symmetrical axis by means of an ARCAM[®] Q10 machine with diameter of 40 mm and length of 230 mm. The chemical composition and the mechanical properties of the EBM Ti6Al4V are summarised in Tables 1 and 2, respectively. The EBM Ti6Al4V presents lower ultimate strength, yield stress and elongation at fracture than the conventional

Table 1
EBM Ti6Al4V chemical composition (%weight).

Chemical composition (wt%)							
Al	V	C	Fe	O	N	H	Ti
6	4	0.03	0.1	0.15	0.01	0.003	Bal

Table 2

EBM and wrought Ti6Al4V mechanical properties.

Material	Young's Modulus [GPa]	Ultimate tensile strength [MPa]	Yield stress [MPa]	Elongation [%]	Hardness [HRC]
EBM Ti6Al4V	118	914	830	13.1	35
Wrought Ti6Al4V	114	940	870	15.0	33

wrought alloy, whereas both the Young's modulus and the hardness are comparable (see Table 2). In general, it can be stated that the EBM technology produces a material with lower ductility than the wrought alloy, which may determine different machinability characteristics in terms of tool wear behaviour and machined surface integrity that are worthwhile to be investigated.

The AM techniques applied to metallic parts produce porous surfaces: consequently, the porous surface of the as-built cylindrical specimens was removed by turning a 1 mm thick layer, which assured the same initial surface characteristics for all the tested samples, with a resulting average surface roughness Ra equal to 1 μm .

2.2. Machining tests

A Mori Seiki NL1500™ CNC lathe was used for the conduction of the semi-finishing turning tests. The cooling system provided with the machine tool was used to fulfil standard flooding (wet turning), whereas a dedicated line was designed to realize the cryogenic cooling. Thanks to its higher cooling capacity compared to other liquefied gasses, as the LCO₂, its lower process consumption and lower production costs, as proved by Pusavec et al. (2014), the LN₂ was used in this work for the cryogenic cooling.

The LN₂ was supplied to the cutting zone at a constant pressure of 15 bar through two external copper nozzles with an internal diameter of 1 mm that directed the flow towards the tool flank and rake faces, as shown in Fig. 1 right. An overview of the experimental set-up adopted for the cryogenic cooling is presented in a work published by the same authors (Bordin et al., 2015a). The standard commercial semi-synthetic cutting fluid Monroe® Astro-Cut HD XBP was mixed with water obtaining a 5% emulsion coolant that was supplied to the cutting zone at a pressure of 5 bar through the cooling system of the machine tool.

A semi-finishing coated tungsten carbide insert CNMG 120404SM-GC1105 supplied by Sandvik-Coromant® was used as cutting tool insert; a TiAlN coating deposited by PVD was chosen as it was proved to help reducing the tendency of the Ti6Al4V alloy to stick on the cutting surfaces during machining processes (Özel et al., 2010; Vinayagamoorthy and Xavier, 2013), thanks to the low friction coefficient and high thermal resistance generated by the presence of aluminium and titanium in the coating (Cantero et al., 2013). The insert geometry has a nose radius of 0.4 mm,

rake angle of 7° and clearance angle of 0° with a chip breaker. The choice of delivering the LN₂ to the cutting zone through external nozzles allowed using the same tool holder for all the tested cooling conditions, mounting a Sandvik-Coromant® PCLNR\R 2020K12 tool holder with an approach angle of 95°. Two levels of the cutting speed and feed rate were tested, namely 50 and 80 m/min, and 0.1 and 0.2 mm/rev, respectively; the depth of cut was kept constant and equal to 0.25 mm. As mentioned before, these parameters can be used in a real industrial scenario when turning AM parts, as a limited amount of machining allowance has to be removed. Since the tool wear directly affects the process costs and the environmental impact (Schultheiss et al., 2013), the turning tests were conducted at fixed time length of 3–8–15 min for each cutting condition, aiming at controlling the efficiency of the cooling conditions on the tool utilization; a fresh cutting edge was used for each trial for a total of 9 trials for each cooling condition. At the end of each turning step, a 15 mm long specimen was cut from the bar and collected, together with the chips and the turning inserts to carry out further investigations. The turning tests were repeated three times for each cutting condition to assure the results repeatability.

2.3. Tool wear and surface integrity measurements

The tool wear was quantified by measuring the standard flank wear width under the tool nose, namely the VB_c parameter according to the standard ISO 3685:1993; the other flank wear parameters, namely VB_B and VB_N , were not considered as the wear of the insert flank face was located under the curved portion of the cutting edge, being the adopted depth of cut smaller than the tool nose radius. A tool wear limit rejecting criterion was chosen by fixing a threshold value for the VB_c parameter equal to 100 μm , which is a conservative condition usually employed in finishing operations for aerospace and automotive components. During the turning tests, the measurement of the VB_c was conducted using a hand-held digital microscope Dino-Lite® AM 413ZT, which has polarization capabilities and high magnification up to 200 \times . Later on, each worn insert was analysed using a FEI QUANTA 450® Scanning Electron Microscope (SEM) equipped with the ETD and BSED detectors. During the SEM analysis, the tool wear modes were identified, and the flank wear width was more accurately measured.

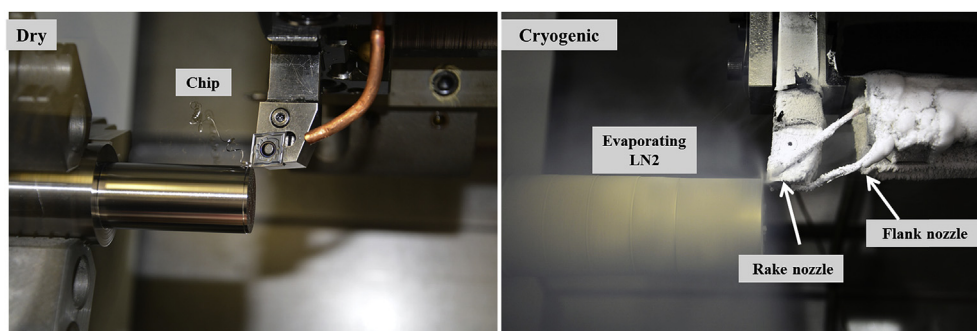


Fig. 1. Semi-finishing turning of EBM Ti6Al4V under dry cutting (left) and cryogenic cooling (right).

The integrity of the machined surfaces was evaluated using different techniques. The surface roughness parameters Ra and Rt (arithmetic mean surface roughness and total height of the roughness profile, respectively) were measured at 5 different positions on the machined surface with a Taylor Hobson-Subtronic 25™ portable roughness tester, the average values were then calculated and plotted for each test trial.

As machining operations are recognised to leave defects on the final surfaces, which can have detrimental effects on the product service life, affecting, in particular, the fatigue life (Ulutan and Ozel, 2011), a SEM analysis was carried out to qualitatively investigate the density and typology of the defects present on the machined surfaces. Moreover, an EDS analysis was conducted to identify the chemical composition of the adhered particles on the machined surfaces, by means of an EDAX® dispersive X-Ray spectroscopy detector installed in the SEM.

2.4. Chip morphology characterization

The collected chips were cut, cold mounted and manually polished according to the standard metallographic preparation procedures and then etched with the Kroll's reagent to evidence the microstructure, allowing, at the same time, a more accurate micro-geometrical characterization of the chip segmentation. The chips microstructure was observed using the Leica MEF4U® optical microscope and their micro-geometry measured by using the imaging software supplied with the microscope.

3. Experimental results and discussion

3.1. Evolution of the tool wear and wear mechanisms

The influence of the cooling strategies on the nose wear parameter VB_c at fixed machining times is shown in Fig. 2, when a cutting speed of 80 m/min and a feed rate of 0.1 mm/rev (Fig. 2a) and 0.2 mm/rev (Fig. 2b) are adopted, respectively. It is worth to underline that, in all the turning trials, the tool rejection criterion, set at 0.1 mm for the VB_c parameter, was never reached.

Moreover, Fig. 2 shows that a significantly lower tool wear was found in case of cryogenic cooling application, which was also evident with a cutting speed of 50 m/min. On the other hand, dry turning produced higher nose wear in comparison with standard wet turning, in particular for the feed rate of 0.2 mm/rev. The flank and nose wear of the tool is usually related to the abrasive action of the workpiece against the tool flank face, which first removes the tool coating and then the substrate particles (Dutta et al., 2013). The addition of mineral oil to the water to generate the emulsion

coolant has the proper function of reducing the friction coefficient that generates at the cutting interfaces and, consequently, of lowering the cutting temperature. It is not surprising that for such cutting parameters, higher values of the flank wear resulted under dry turning when the most severe cutting parameters were adopted. Conversely, dry turning became competitive with the conventional flooding when the lowest feed rate was applied, leading to comparable or even lower values of the VB_c (see Fig. 2a); this may be ascribed to the lower friction forces and temperatures generated at the tool-workpiece interface in comparison to those obtained at the highest feed rate.

The SEM analysis of the worn tools highlighted the main tool wear mechanisms occurring when turning the EBM Ti6Al4V under wet, cryogenic and dry cooling conditions. Adhesion was the main wear mechanism, confirming the sticky tendency of the EBM Ti6Al4V, and it was noticed in all the turning tests, as shown in Fig. 3 where the worn tools are presented when a cutting speed of 80 m/min and a feed rate of 0.2 mm/rev were adopted, after 15 min of turning. Even if the microstructure of the EBM Ti6Al4V is quite different than the one of the wrought Ti6Al4V, the affinity among its main chemical elements with those composing the tool insert (mainly Ti, Al, W, Co), its low thermal conductivity and the high specific cutting forces reached during the machining process, favour the adhesive wear mechanism as it happens in case of machining the wrought Ti6Al4V (Hartung et al., 1982).

The adhesion of Ti6Al4V layers on the tool faces when machining with coated or uncoated tungsten carbide inserts have been extensively investigated also when using alternative cooling strategies, such as cryogenic cooling (Courbon et al., 2013), High Pressure Water Jet Assistance (HPWJA) and Minimum Quantity Lubrication (MQL) (Ezugwu, 2005). In this study, the adhesion occurrence is evident from the presence of the pastel grey areas on the SEM images obtained with the BSED detector (see Fig. 3). This tool wear mechanism led to the formation of the Built-Up-Edge (BUE) and the crater wear on the tool rake face in case of wet and dry machining (see Fig. 3a and b). Since the early stages of the cutting process, cratering occurred during dry and wet turning when the most severe cutting parameters were adopted because of the higher specific cutting forces and temperatures; on the contrary, it was never observed with the LN2 application (see Fig. 3c). Bordin et al. (2015b) measured the cutting temperatures when turning the EBM Ti6Al4V in semi-finishing turning conditions under dry and cryogenic cooling adopting an uncoated tungsten carbide insert with similar cutting process parameters. The maximum cutting temperature on the tool rake face resulted to be around 380 °C during dry turning, whereas a lower value around 120 °C was measured under cryogenic cooling. Even if no measurements

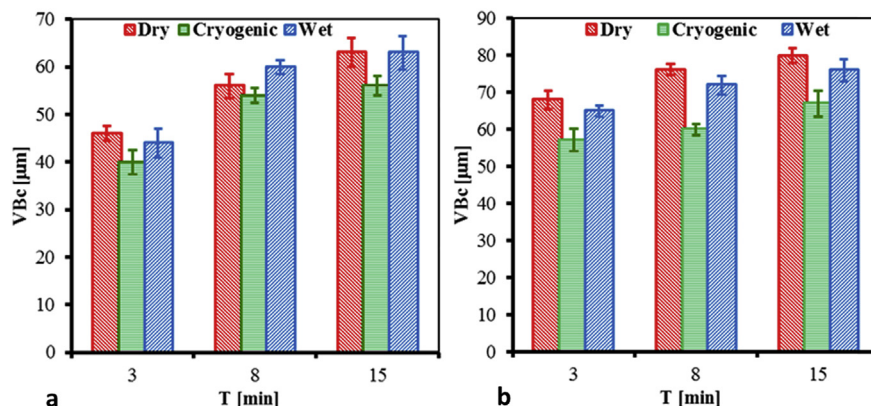


Fig. 2. Nose wear VB_c as a function of the machining time and cooling strategies when adopting a cutting speed of 80 m/min and a feed rate of: a) 0.1 mm/rev and b) 0.2 mm/rev.

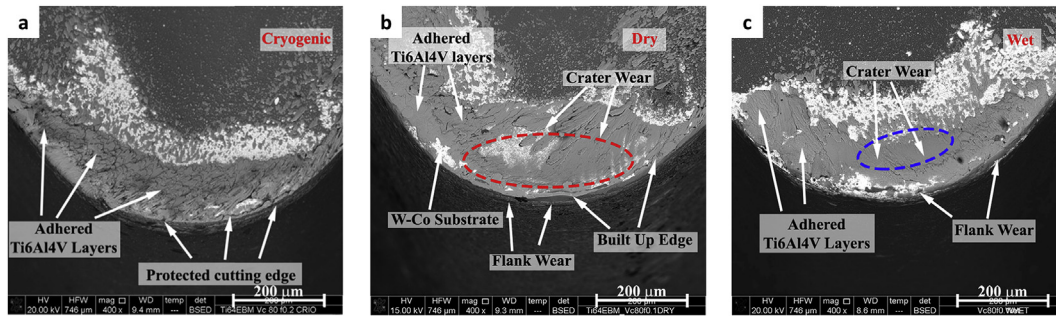


Fig. 3. SEM images of the worn tools after 15 min of turning when adopting a cutting speed of 80 m/min and a feed rate of 0.2 mm/rev under: a) cryogenic cooling, b) dry cutting, and c) wet cutting.

of the cutting temperature were carried out in this study, it can be reasonably assumed that its values under wet turning might position between those measured under dry and cryogenic cooling conditions. Cratering is a well-known adhesion-diffusion wear process provoked by the continuous formation and breakage of strong bonds between the sliding surface of the chips and the already adhered workpiece layers or fresh tool substrate particles. The crater formation is strongly dependent on the temperatures reached at the tool-workpiece interface rather than the specific normal pressure (Venugopal et al., 2007). Thus, the higher the temperatures the higher the tendency of the workpiece material adhesion on the tool cutting faces. On this basis, the higher amounts of adhered material noticed on the tool faces and the occurrence of cratering during dry and wet turning are directly correlated to the high temperatures reached in the cutting zone; in particular, the avoidance of the application of a cutting fluid speeds up the adhesive wear rate, leading to wider craters as visible in Fig. 3b. The SEM analysis of the worn tools revealed an intense presence of adhered layers even on the cutting edge and on the rake face, with more regular and intact geometries when applying the LN₂. The presence of these layers tends to protect the tool substrate when the coating is abraded during the early stages of the machining process, providing, at the same time, a thermal barrier for the substrate. Nonetheless, higher wear rates were reached during dry and wet cooling conditions due to the higher temperatures; hence the cutting edge was more subjected to unpredictable detachments of fragments suffering more severely the rubbing effect of the workpiece against the tools substrate, thus affecting the tool flank wear resistance.

From an environmental point of view, cryogenic cooling meets the increasing demand for a more sustainable manufacturing since it increases the tool life, and thus limits the number of used cutting tools. When a feed rate of 0.1 mm/rev is set, dry turning becomes a sustainable alternative to the standard wet machining thanks to the

comparable values of the nose wear.

3.2. Surface integrity

The average values of the mean surface roughness R_a and the total height of the roughness profile R_t are listed in Table 3, whereas in Fig. 4 the cooling strategy effect on the mean surface roughness after 8 min of turning is shown. As expected, the surface roughness is mainly influenced by the feed rate: the higher the feed rate the higher the roughness, whereas the increase of the cutting speed affects it to a less extent. This behaviour is evident for the feed rate of 0.2 mm/rev, where the surface roughness varies in dry condition from 1.86 to 2.06 μm at cutting speed of 50 and 80 m/min respectively. However, this trend is not respected in case of a feed rate equal to 0.1 mm/rev: as reported in Table 3, the increase of the

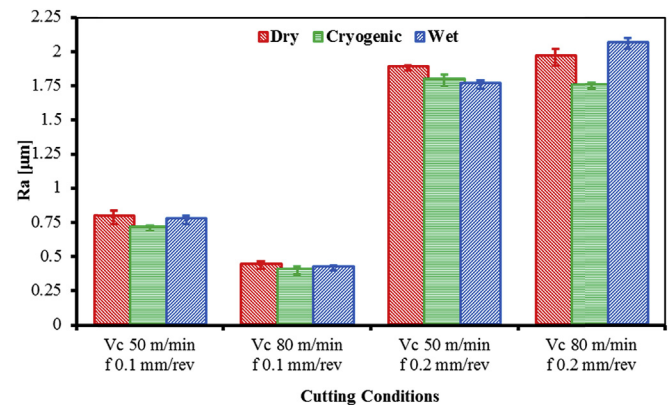


Fig. 4. Effect of the cooling strategies on the mean surface roughness R_a after 8 min of turning.

Table 3

Average values of the roughness parameters R_a and R_t .

Cutting parameters	Time [min]	$R_{a,dry}$ [μm]	$R_{a,cryo}$ [μm]	$R_{a,wet}$ [μm]	$R_{t,dry}$ [μm]	$R_{t,cryo}$ [μm]	$R_{t,wet}$ [μm]
Vc 50 m/min f 0.1 mm/rev	3	0.76	0.82	0.64	3.48	4.15	2.88
	8	0.79	0.81	0.71	3.53	3.85	3.12
	15	0.77	0.81	0.74	3.56	3.89	3.46
Vc 50 m/min f 0.2 mm/rev	3	1.86	1.78	1.49	7.01	7.13	6.56
	8	1.88	1.79	1.75	7.84	8.46	6.90
	15	1.81	1.72	2.13	7.61	7.37	7.99
Vc 80 m/min f 0.1 mm/rev	3	0.49	0.39	0.74	2.98	2.09	3.55
	8	0.44	0.42	0.42	2.06	4.29	2.54
	15	0.46	0.61	0.55	2.71	3.43	2.20
Vc 80 m/min f 0.2 mm/rev	3	2.06	1.32	2.10	7.03	6.18	7.90
	8	1.96	1.75	2.06	8.54	7.03	8.08
	15	2.10	1.82	2.14	8.45	6.94	8.22

cutting speed determines a decrease of Ra. This may be ascribed to the fact that the cutting conditions of 0.1 mm/rev and 50 m/min are very close to the lower limit parameters recommended by the tool manufacturer, which may have an adverse effect on the machined surface roughness. It is evident a reduction of the Ra values when the cryogenic cooling is applied at the most severe cutting parameters, namely a cutting speed of 80 m/min and a feed rate of 0.2 mm/rev, whereas negligible differences result for the lowest feed rate. At the most severe cutting conditions, the use of LN2 determines lower tool wear in terms of both crater and flank wear, preserving the cutting edge geometry. Generally, the more severe the tool wear the poorer the surface quality, thus lower values of Ra and Rt were measured for the cryogenically machined samples as can be seen in Table 3. If the cutting speed is reduced to 50 m/min, the LN2 application still led to beneficial effects inducing lower values of Ra and Rt, even if values closer to the cases of wet and dry turning were found.

The surface roughness is deeply influenced by the tool flank wear; however, the tool wear analysis pointed out that no direct contact between the workpiece and the tool flank occurred as great amounts of adhered workpiece material were present, thus limiting the occurrence of the abrasive wear mechanism. This phenomenon strongly reduces the effects of the adopted cooling strategies in case of semi-finishing machining compared to most of the published works on rough machining of the wrought Ti6Al4V. In case of rough machining, the rapid wear rate provokes significant differences among the different cooling conditions, while, in the case of semi-finishing machining, negligible differences were found for the lowest feed rate, even for longer turning lengths.

From an environmental perspective, both dry cutting and cryogenic cooling are feasible strategies to obtain surfaces characterized by acceptable roughness, but a more comprehensive analysis of the surface characteristics is needed to assess their possible implementation in the biomedical field.

On these bases, a SEM analysis of the surface damage resulting from the turning process was carried out. The extent of the surface damage that occurs during machining and how it develops are important information since the in-service performances of the machined components are strongly influenced by the state of the surface layers (Jouini et al., 2013). In literature, a strong emphasis

has been paid to characterize surface damages generating during rough milling and turning of wrought titanium and nickel alloys (Ulutan and Ozel, 2011; Zhou et al., 2012), but very few works are available about finishing turning of AM alloys (Axinte et al., 2006). Many variables are involved, such as the ductility of the workpiece material, its microstructure, the tool mechanical properties, and the thermo-mechanical conditions arising during the process; furthermore, the tool wear and cutting parameters significantly affect the machined surface damage (Zou et al., 2009). An overview of the main typologies of surface defects generated under the tested cooling conditions is presented in Fig. 5.

In general, material side flow, double feed marks, long grooves and micro-particles adhered on the machined surface were found under wet turning as can be seen in Fig. 5a and d, with a greater density for the highest feed rate and for longer turning lengths, whereas the influence of the cutting speed was weak. The material side flow can be ascribed to the plastic deformation of the surface material induced by the tool motion, enhanced by an increased plasticity provoked by the higher temperatures reached when the most severe cutting parameters were adopted. Long straight grooves can be also noticed between two consecutive feed marks in all the samples machined under wet conditions, meaning that a ploughing action exerted by the cutting edge took place. According to Zhou et al. (2012), these grooves are generated by small fragments of the BUE that are randomly detached by the rubbing action, hence, when they pass below the tool flank face, they leave grooves on the softer underlying material. Moreover, the great amount of adhered material developing in all the turning tests left particles welded on the surface, as can be noted in Fig. 6. On the same figure, randomly oriented micro-scratches are visible, generated by the chip entanglements occurred during wet turning. Cleaner and more undamaged surfaces resulted when a feed rate equal to 0.1 mm/rev was adopted.

Ti6Al4V is characterized by a poor thermal conductivity compared to other metal alloys (Krämer et al., 2014): as a consequence, the thermal flux that is dissipated through the workpiece encounters more resistance, and higher temperatures are concentrated on its surface. If no coolant is applied, higher temperatures are reached at the workpiece–tool interface making the material softer, thus leading to more surface defects in comparison to wet

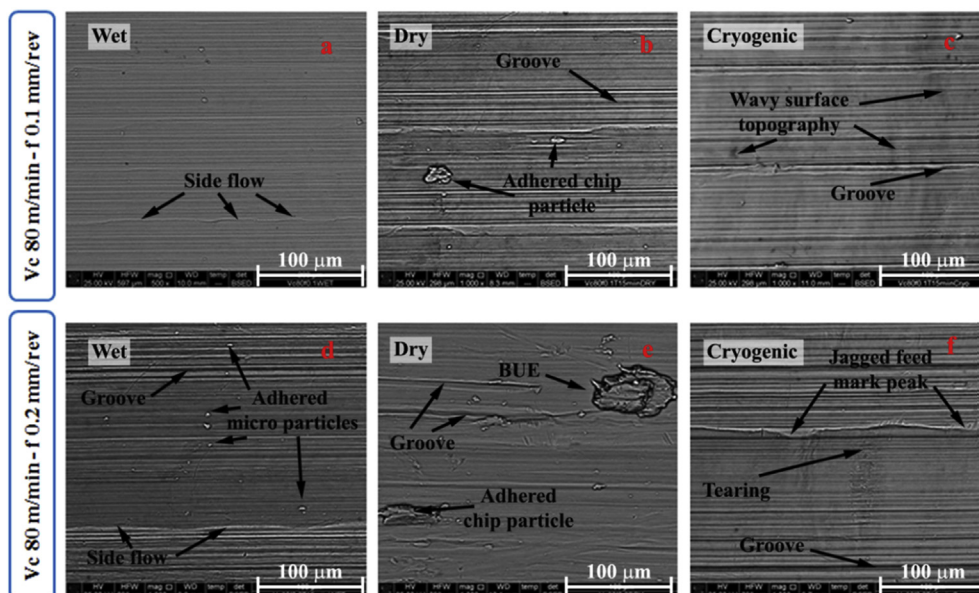


Fig. 5. Main surface defects after 8 min of turning adopting wet, dry and cryogenic cooling strategies.

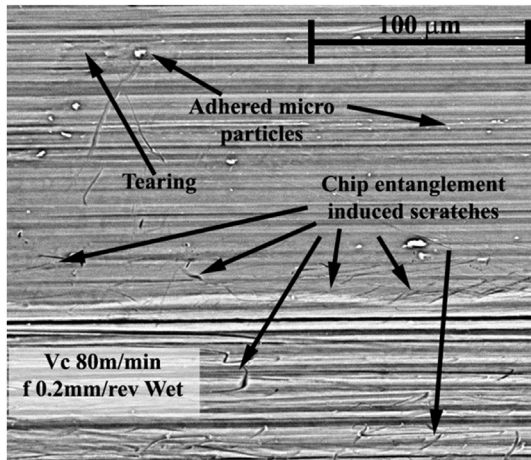


Fig. 6. Scratches and adhered particles provoked by chip entanglements after 8 min of wet cutting.

turning carried out at the same cutting parameters. In Fig. 5b and e, wider adhered chip fragments attached on the machined surfaces are present, especially for the most severe cutting parameters. Under dry cutting, BUE, adhered chip fragments, long grooves, folds, severe material side flow and smeared material were found as main surface defects. The feed rate played a major role, increasing the size and density of the surface defects compared to wet turning. A portion of the BUE adhered on the machined surface and the EDS analysis reported in Fig. 7 confirms its chemical composition, being the same of the workpiece material. When portions of BUE were deposited on the surface, they were dragged on the fresh surface leaving long grooves as can be seen in Fig. 5e. During dry turning, chip entanglements occurred, and due to the higher temperatures that developed, chip fragments tended to weld onto the surface.

Fig. 5c and f shows the machined surfaces generated under cryogenic cooling conditions evidencing the effect of the feed rate when a cutting speed of 80 m/min was adopted. The main peculiarities are the wavy surface topography along the cutting speed direction (normal to the feed marks) and the jagged feed marks peaks. These characteristics were observed even for the lowest cutting speed and regardless of the tool wear condition. Since the workpiece was frozen during the machining tests due to the LN₂ application, the plasticity of the alloy was noticeably reduced limiting its capacity to be deformed by the tool nose passage and, therefore, to form regular feed marks. This low plasticity of the surface layers is further proved by the presence of tears and wrinkles inside the feed mark valleys. A snapshot of the surface defects occurred when applying cryogenic cooling is presented in Fig. 8. In comparison to the surface defects found in case of wet and dry machining, cleaner surfaces were observed, showing fewer adhered particles and chip fragments, less side flow and BUE, thanks to the reduced material plasticity provoked by the cryogenic thermal conditions.

Shorter machining operations would limit cooling of the workpiece and, therefore, would reduce the waviness of the machined surfaces: this is feasible in case of machining AM components since very few cutting passes are necessary to finish the already near-net-shape geometries.

3.3. Chip morphology

The chip control is of paramount importance during a machining process in order to achieve both a stable breakability and an easy disposal. In general, long chips should be avoided to

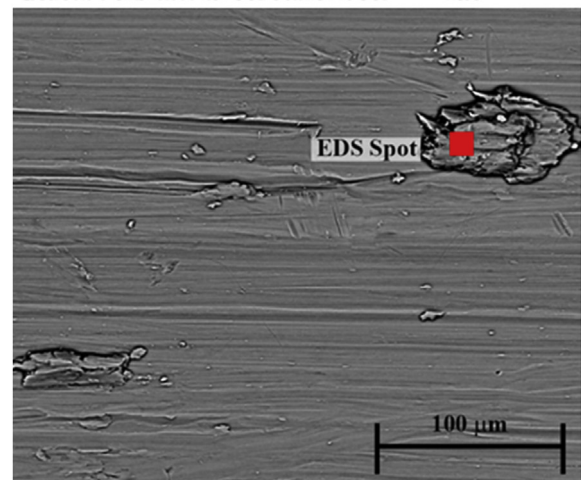
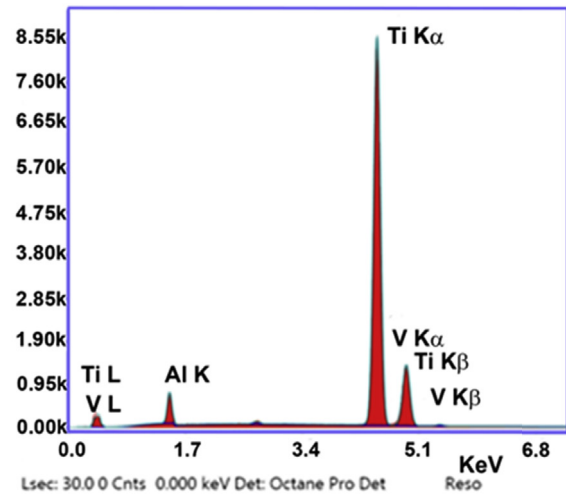


Fig. 7. EDS analysis of BUE fragments adhered on the machined surface after 8 min of dry cutting.

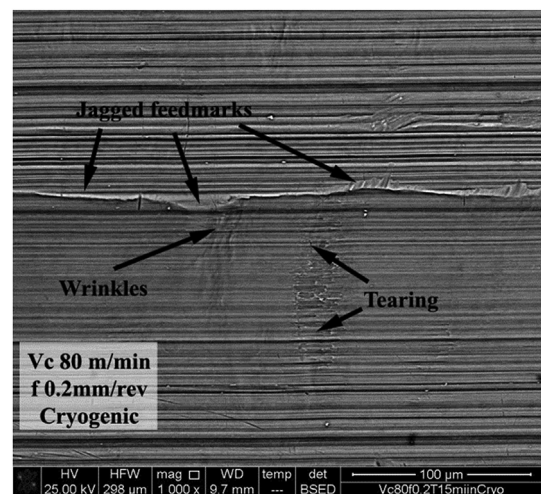


Fig. 8. Main surface defects after 8 min of cryogenic cutting.

prevent entanglements around the workpiece or along the chip conveyor leading to workpiece and machine tool damages or even production stops to evacuate the chips. Further information about the feasibility and sustainability of dry cutting and cryogenic

cooling strategies can be gained by the chip morphology analysis. Fig. 9 shows the chips morphology after 8 min of cutting, for the two levels of the feed rate at a fixed cutting speed of 80 m/min.

Since the tool wear was limited for all the cutting parameters tested in this work, no significant variations in terms of chip morphology were noticed at different turning times. On the contrary, a significant variation of both the chip size and morphology is noticeable when varying the cooling conditions. Frequent chip entanglements occurred during dry turning because the chip breaker exerted no breaking action due to the low depth of cut. The chips presented a snarled ribbon morphology for the lowest feed rate that changed to a long helical one for the highest feed rate, as shown in Fig. 9b and e. The cutting temperatures reached under these conditions facilitated the adhesion of the chip fragments on the machined surface as discussed in the previous paragraph. It is noteworthy that, under semi-finishing turning, the chip cross section is generally small, hence, for ductile alloys such as the Ti6Al4V, the chips show a great bending capacity leading to a poor breakability (Pusavec et al., 2015). In case of wet turning, the chip morphology changed noticeably as can be seen in Fig. 9c and f appearing as snarled tubes for a feed rate of 0.1 mm/rev, while long tubular chips resulted for a feed rate of 0.2 mm/rev. Thanks to the mechanical action exerted by the coolant flow stream, shorter chips were generated than in case of dry turning when the smallest feed rate was adopted, but less beneficial effects were noticed for the highest feed rate due to the higher chip thickness, leading to the formation of 200 mm long chip segments. In addition, the chip radius drastically increased in comparison to dry turning, damaging both the cutting tool and the machined surface, as shown in Fig. 5.

A better chip control was achieved when applying the cryogenic cooling, because of the material plasticity drop due to the lower cutting temperatures, which reduced the ductility and the bending capacity of the material involved in the chip formation. Fig. 9a and d shows that long helical chips with an average diameter of 2 mm formed at the lowest feed rate, while 20 mm long snarled helical chips were collected at the highest feed rate. In both cases, no chip entanglements formed around the tool holder enhancing the chips evacuation from the working area. Even though no comparable works can be found in literature about machining the EBM Ti6Al4V, these findings are in accordance with other published works on the effect of cryogenic cooling on the chip morphology when turning wrought nickel and titanium alloys. In a recent work, Pusavec et al. (2015) found a better chip breakability when turning the wrought

Inconel 718 under cryogenic cooling, with even better results when coupled with the MQL. Pradeep Kumar and Dilip Jerold (2013) noticed a better chip control and breakability during turning the wrought Ti6Al4V when applying the LN₂ compared to the CO₂. In both works, the Authors considered the low temperatures reached during cutting as the main driving force for a better chip breakability. With the aim at better understanding the effect of the cooling strategy on the chip morphology, the chips were collected, mounted, polished and etched to characterize their cross section geometry. 30 measurements of the distance between serrations d_s (see Fig. 10) and of the chip thickness c_t were carried out for each cutting condition. The averaged measurements are summarised in Figs. 11 and 12 for a cutting length of 8 min, respectively. Serrated



Fig. 10. Cross-section of the chip generated under cryogenic cooling with indication of the measured chip features.

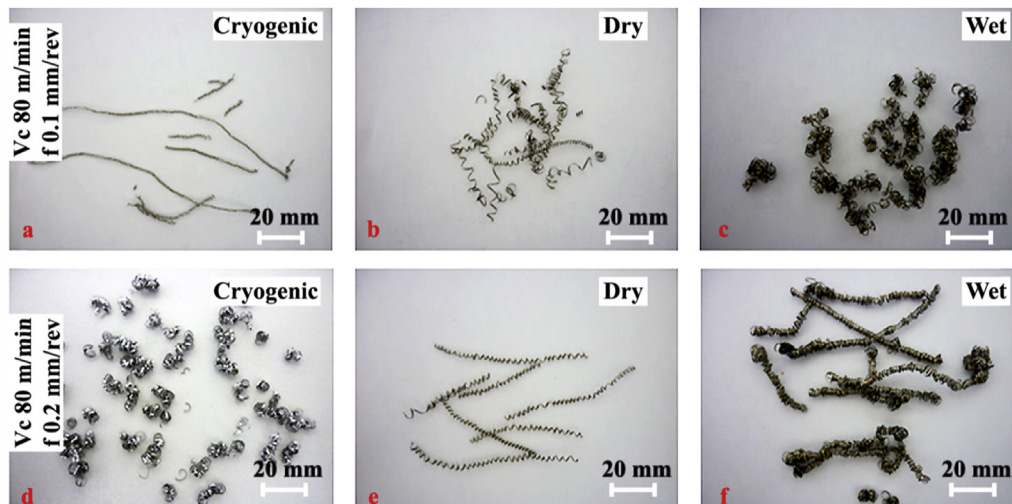


Fig. 9. Chip morphology under cryogenic, dry and wet turning conditions after 8 min of cutting and for a cutting speed of 80 m/min.

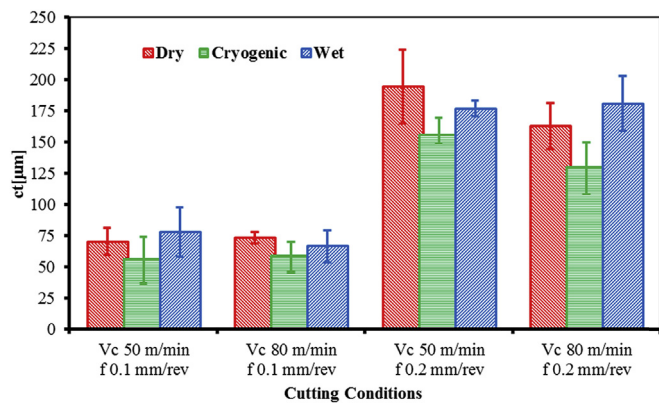


Fig. 11. Effect of the cooling strategies on the chip thickness after 8 min of cutting.

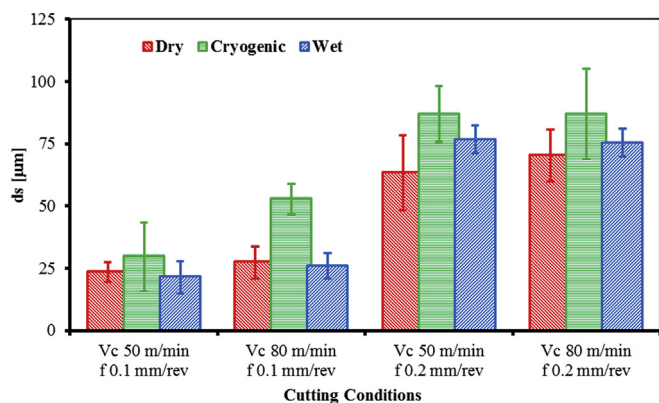


Fig. 12. Effect of the cooling strategies on the distance between serrations for the chips formed after 8 min of cutting.

chips resulted regardless of the cooling strategy, and the micro-structural analysis proved that the chip segmentation consisted of a cracking–shear banding mechanism, as can be noticed in Fig. 10, where a crack and an Adiabatic Shear Band (ABS) are highlighted between two consecutive chip peaks. The serrated chips were more regular for the highest feed rate regardless of the cooling strategy. The chip segmentation mechanism in machining Ti6Al4V is boosted by the cutting temperature and by the amount of deformation induced on the primary shear zone (Ye et al., 2013), hence, for the low depth of cut applied in this work, a higher segmentation tendency for the most severe cutting parameters is consistent with the literature records. The application of flood coolants in turning the EBM Ti6Al4V did not significantly affect the cross section geometry of the chip, and no significant discrepancies can be found if the error bands of the results are taken into account. Apart from the scatter in the measurements, which is common in this type of investigation (Bermingham et al., 2012), the marginal differences in the cutting temperatures between dry and wet turning for the low depth of cut here adopted can have limited the effects of the flood coolant on the chip segmentation mechanism. On the other hand, the cryogenic cooling influenced this phenomenon as can be appreciated from the measurements of the chip thickness and the distance between serrations (see Figs. 11 and 12). A chip thickness reduction is noticed mainly for the highest feed rate, whereas for all the cutting parameters combinations, greater distances between serrations were found.

From a sustainable point of view, a reduction of the chip thickness is important because thinner chips allow more space for cooling the cutting zone compared to thicker chips that tend to

insulate the cutting zone from external coolants. Moreover, shorter chips are less hazardous to machine operators and are more convenient to dispose.

4. Conclusions

The paper proved the feasibility of replacing emulsion cutting fluids with more sustainable alternatives when machining the Ti6Al4V alloy produced by the Additive Manufacturing technology known as Electron Beam Melting. The effects of the cooling strategy and cutting parameters (namely the cutting speed and the feed rate) on the tool wear, surface integrity, and chip morphology were investigated. The main findings of this investigation can be summarised as follows:

- The LN2 application gave the lowest tool wear (lowest nose wear V_{bc} and avoidance of cratering) for all the tested cutting parameters, leading to an extension of the tool life and a reduced waste of cutting tools.
- For the lowest feed rate, dry machining led to tool wear values comparable to those of wet cutting, thanks to the severe adhesion of the workpiece material on the tool that limited the effect of the abrasive wear; on the contrary, when the feed rate was increased, dry machining led to severe cratering.
- The cooling conditions did not affect the quality of the machined surfaces when the lowest feed rate was set regardless of the cutting speed, whereas sensible improvements were assured by the LN2 application for the most severe cutting parameters, thanks to a lower nose wear.
- Cryogenic cooling led to cleaner machined surfaces with fewer adhered particles than dry and wet machining; however, due to the lower plasticity of the material induced by the lower cutting temperatures, the machined surfaces were wavier with the presence of jagged feed marks.
- The chip morphology changed considerably with the applied cooling strategy. Cryogenic cooling enhanced the chip breakability due to the low ductility of the chips cooled by the LN2 flow streams, thus avoiding entanglements around the tool holder, which, instead, occurred during wet and dry turning, being more hazardous for the operator and more complicated to dispose.
- From an environmental point of view, cryogenic cooling is more suitable than dry machining to be implemented in machining EBM Ti6Al4V, fulfilling an overall potential reduction of the production costs and environmental impact if applied in the biomedical field; nonetheless, further researches need to be carried out to evaluate the impact of the LN2 application to the geometrical tolerances in machining biomedical components.

References

- Axinte, D.A., Andrews, P., Li, W., Gindy, N., Withers, P.J., 2006. Turning of advanced Ni based alloys obtained via powder metallurgy route. *CIRP Ann. - Manuf. Technol.* 55, 117–120. [http://dx.doi.org/10.1016/S0007-8506\(07\)60379-5](http://dx.doi.org/10.1016/S0007-8506(07)60379-5).
- Baumers, M., Dickens, P., Tuck, C., Hague, R., 2015. The cost of additive manufacturing: machine productivity, economies of scale and technology-push. *Technol. Forecast. Soc. Change.* <http://dx.doi.org/10.1016/j.techfore.2015.02.015>.
- Bennett, E.O., 1983. Water based cutting fluids and human health. *Tribol. Int.* 16, 133–136. [http://dx.doi.org/10.1016/0301-679X\(83\)90055-5](http://dx.doi.org/10.1016/0301-679X(83)90055-5).
- Bermingham, M.J., Palanisamy, S., Kent, D., Dargusch, M.S., 2012. A comparison of cryogenic and high pressure emulsion cooling technologies on tool life and chip morphology in Ti-6Al-4V cutting. *J. Mater. Process. Technol.* 212, 752–765. <http://dx.doi.org/10.1016/j.jmatprotec.2011.10.027>.
- Bordin, A., Imbrogno, S., Rotella, G., Bruschi, S., Ghiotti, A., Umbrello, D., 2015a. Finite element simulation of semi-finishing turning of Electron Beam melted Ti6Al4V under dry and cryogenic cooling. *Procedia CIRP* 31, 551–556. <http://dx.doi.org/10.1016/j.procir.2015.03.040>.
- Bordin, A., Bruschi, S., Ghiotti, A., Bariani, P.F., 2015b. Analysis of tool wear in cryogenic machining of additive manufactured Ti6Al4V alloy. *Wear* 328–329,

- 89–99. <http://dx.doi.org/10.1016/j.wear.2015.01.030>.
- Cantero, J.L., Díaz-Alvarez, J., Miguélez, M.H., Marín, N.C., 2013. Analysis of tool wear patterns in finishing turning of Inconel 718. *Wear* 297, 885–894. <http://dx.doi.org/10.1016/j.wear.2012.11.004>.
- Chen, Q., Thous, G.A., 2015. Metallic implant biomaterials. *Mater. Sci. Eng. R. Rep.* 87, 1–57. <http://dx.doi.org/10.1016/j.mser.2014.10.001>.
- Courbon, C., Pusavec, F., Dumont, F., Rech, J., Kopac, J., 2013. Tribological behaviour of Ti6Al4V and Inconel718 under dry and cryogenic conditions - application to the context of machining with carbide tools. *Tribol. Int.* 66, 72–82. <http://dx.doi.org/10.1016/j.triboint.2013.04.010>.
- Debnath, S., Reddy, M.M., Yi, Q.S., 2014. Environmental friendly cutting fluids and cooling techniques in machining: a review. *J. Clean. Prod.* 83, 33–47. <http://dx.doi.org/10.1016/j.jclepro.2014.07.071>.
- Devillez, A., Le Coz, G., Dominiak, S., Dudzinski, D., 2011. Dry machining of Inconel 718, workpiece surface integrity. *J. Mater. Process. Technol.* 211, 1590–1598. <http://dx.doi.org/10.1016/j.jmatprotec.2011.04.011>.
- Dudzinski, D., Devillez, A., Moufki, A., Larrouquère, D., Zerrouki, V., Vigneau, J., 2004. A review of developments towards dry and high speed machining of Inconel 718 alloy. *Int. J. Mach. Tools Manuf.* 44, 439–456. [http://dx.doi.org/10.1016/S0890-6955\(03\)00159-7](http://dx.doi.org/10.1016/S0890-6955(03)00159-7).
- Dutta, S., Kanwat, a, Pal, S.K., Sen, R., 2013. Correlation study of tool flank wear with machined surface texture in end milling. *Meas. J. Int. Meas. Confed.* 46, 4249–4260. <http://dx.doi.org/10.1016/j.measurement.2013.07.015>.
- Environmental Protection Agency. EPA. <www.epa.gov> (accessed 20.07.15).
- Ezugwu, E.O., 2005. Key improvements in the machining of difficult-to-cut aerospace superalloys. *Int. J. Mach. Tools Manuf.* 45, 1353–1367. <http://dx.doi.org/10.1016/j.ijmachtools.2005.02.003>.
- Ezugwu, E.O., Wang, Z.M., 1997. Titanium alloys and their machinability. *J. Mater. Process. Technol.* 68, 262–274. [http://dx.doi.org/10.1016/S0924-0136\(96\)00030-1](http://dx.doi.org/10.1016/S0924-0136(96)00030-1).
- Fratila, D., 2010. Macro-level environmental comparison of near-dry machining and flood machining. *J. Clean. Prod.* 18, 1031–1039. <http://dx.doi.org/10.1016/j.jclepro.2010.01.017>.
- Gao, W., Zhang, Y., Ramanujan, D., Ramani, K., Chen, Y., Williams, C.B., Wang, C.C.L., Shin, Y.C., Zhang, S., Zavattieri, P.D., 2015. The status, challenges, and future of additive manufacturing in engineering. *Comput. Des.* <http://dx.doi.org/10.1016/j.cad.2015.04.001>.
- Hartung, P.D., Kramer, B.M., von Turkovich, B.F., 1982. Tool wear in titanium machining. *CIRP Ann. - Manuf. Technol.* 31, 75–80. [http://dx.doi.org/10.1016/S0007-8506\(07\)63272-7](http://dx.doi.org/10.1016/S0007-8506(07)63272-7).
- Hong, S.Y., Ding, Y., Jeong, W.C., 2001. Friction and cutting forces in cryogenic machining of Ti-6Al-4V. *Int. J. Mach. Tools Manuf.* 41, 2271–2285. [http://dx.doi.org/10.1016/S0890-6955\(01\)00029-3](http://dx.doi.org/10.1016/S0890-6955(01)00029-3).
- Hosseini Tazehkandi, A., Pilehvarian, F., Davoodi, B., 2014. Experimental investigation on removing cutting fluid from turning of Inconel 725 with coated carbide tools. *J. Clean. Prod.* 80, 271–281. <http://dx.doi.org/10.1016/j.jclepro.2014.05.098>.
- International Standard Organization, 1993. ISO 3686 Tool-life Testing with Single-point Turning Tools.
- Jouini, N., Revel, P., Mazeran, P.E., Bigerelle, M., 2013. The ability of precision hard turning to increase rolling contact fatigue life. *Tribol. Int.* 59, 141–146. <http://dx.doi.org/10.1016/j.triboint.2012.07.010>.
- Krämer, A., Klocke, F., Sangermann, H., Lung, D., 2014. Influence of the lubricoolant strategy on thermo-mechanical tool load. *CIRP J. Manuf. Sci. Technol.* 7, 40–47. <http://dx.doi.org/10.1016/j.cirpj.2013.09.001>.
- National Council for Advanced Manufacturing. NACFAM. <www.nacfam.org> (Accessed 20 July 2015).
- Ozcelik, B., Kuram, E., Huseyin Cetin, M., Demirbas, E., 2011. Experimental investigations of vegetable based cutting fluids with extreme pressure during turning of AISI 304L. *Tribol. Int.* 44, 1864–1871. <http://dx.doi.org/10.1016/j.triboint.2011.07.012>.
- Özel, T., Sima, M., Srivastava, A.K., Kaftanoglu, B., 2010. Investigations on the effects of multi-layered coated inserts in machining Ti-6Al-4V alloy with experiments and finite element simulations. *CIRP Ann. - Manuf. Technol.* 59, 77–82. <http://dx.doi.org/10.1016/j.cirp.2010.03.055>.
- Pradeep Kumar, M., Dilip Jerold, B., 2013. Effect of cryogenic cutting coolants on cutting forces and chip morphology in machining Ti-6Al-4V alloy. *AJSTPME* 6 (2), 1–7.
- Pusavec, F., Krajcnik, P., Kopac, J., 2010. Transitioning to sustainable production - Part I: application on machining technologies. *J. Clean. Prod.* 18, 174–184. <http://dx.doi.org/10.1016/j.jclepro.2009.08.010>.
- Pusavec, F., Deshpande, A., Yang, S., M'Saoubi, R., Kopac, J., Dillon, O.W., Jawahir, I.S., 2014. Sustainable machining of high temperature Nickel alloy - Inconel 718: Part 1-Predictive performance models. *J. Clean. Prod.* 81, 255–269. <http://dx.doi.org/10.1016/j.jclepro.2014.06.040>.
- Pusavec, F., Deshpande, A., Yang, S., M'Saoubi, R., Kopac, J., Dillon, O.W., Jawahir, I.S., 2015. Sustainable machining of high temperature Nickel alloy – Inconel 718: part 2 – chip breakability and optimization. *J. Clean. Prod.* 87, 941–952. <http://dx.doi.org/10.1016/j.jclepro.2014.10.085>.
- Schultheiss, F., Zhou, J., Gröntoft, E., Ståhl, J.E., 2013. Sustainable machining through increasing the cutting tool utilization. *J. Clean. Prod.* 59, 298–307. <http://dx.doi.org/10.1016/j.jclepro.2013.06.058>.
- Shao, H., Li, L., Liu, L.J., Zhang, S.Z., 2013. Study on machinability of a stellite alloy with uncoated and coated carbide tools in turning. *J. Manuf. Process* 15, 673–681. <http://dx.doi.org/10.1016/j.jmapro.2013.10.001>.
- Ulutan, D., Özel, T., 2011. Machining induced surface integrity in titanium and nickel alloys: a review. *Int. J. Mach. Tools Manuf.* 51, 250–280. <http://dx.doi.org/10.1016/j.ijmachtools.2010.11.003>.
- UNICED, 1992. Agenda 21: Programme of Action for Sustainable Development. United Nations, New York, USA.
- Venugopal, K.A., Paul, S., Chattopadhyay, A.B., 2007. Growth of tool wear in turning of Ti-6Al-4V alloy under cryogenic cooling. *Wear* 262, 1071–1078. <http://dx.doi.org/10.1016/j.wear.2006.11.010>.
- Vinayagamoorthy, R., Xavier, M.A., 2013. Dry machining of Ti-6Al-4V using PVD coated tools. *Int. J. Appl. Eng. Res.* 8, 1373–1381.
- Weinert, K., Inasaki, I., Sutherland, J.W., Wakabayashi, T., 2004. Dry machining and Minimum quantity lubrication. *CIRP Ann. - Manuf. Technol.* 53, 511–537. [http://dx.doi.org/10.1016/S0007-8506\(07\)60027-4](http://dx.doi.org/10.1016/S0007-8506(07)60027-4).
- Ye, G.G., Xue, S.F., Jiang, M.Q., Tong, X.H., Dai, L.H., 2013. Modeling periodic adiabatic shear band evolution during high speed machining Ti-6Al-4V alloy. *Int. J. Plast.* 40, 39–55. <http://dx.doi.org/10.1016/j.ijplas.2012.07.001>.
- Yildiz, Y., Nalbant, M., 2008. A review of cryogenic cooling in machining processes. *Int. J. Mach. Tools Manuf.* 48, 947–964. <http://dx.doi.org/10.1016/j.ijmachtools.2008.01.008>.
- Zhou, J.M., Bushlya, V., Stahl, J.E., 2012. An investigation of surface damage in the high speed turning of Inconel 718 with use of whisker reinforced ceramic tools. *J. Mater. Process. Technol.* 212, 372–384. <http://dx.doi.org/10.1016/j.jmatprotec.2011.09.022>.
- Zou, B., Chen, M., Huang, C., An, Q., 2009. Study on surface damages caused by turning NiCr20TiAl nickel-based alloy. *J. Mater. Process. Technol.* 209, 5802–5809. <http://dx.doi.org/10.1016/j.jmatprotec.2009.06.017>. <http://www.epa.gov/>.